Available online at www.sciencedirect.com

ScienceDirect

IFAC Papers Online CONFERENCE PAPER ARCHIVE

IFAC PapersOnLine 55-10 (2022) 1031–1036

Conoscopic Holography feasibility for form error in-situ monitoring in Additive Manufacturing

Peña, F.* Fernández, A.* Zapico, P.* Valiño, G.* Rico, J. C.*

** Department of Construction and Manufacturing Engineering, University of Oviedo, 33203 Gijón Spain (penafernando@uniovi.es)*

Abstract: The lack of standardization and the low quality of parts produced by Additive Manufacturing requires in certain cases the use of in-situ monitoring techniques based on the use of different types of sensors, each of which has advantages and disadvantages depending on the type and nature of the signatures to be analyzed. Therefore, in this work the feasibility of Conoscopic Holography (CH) technology is analyzed for in-situ monitoring of form errors that take place during the creation of each layer in an AM process. The results obtained using this sensor are compared to those of a Coordinate Measuring Machine used as ground truth. The CH sensor is also compared to a Contact Image Sensor in terms of metrological performance, proving the former to be more suitable and versatile for monitoring this type of errors.

Keywords: Conoscopic Holography, Contact Image Sensor, Additive Manufacturing, layer form error, in-situ monitoring

1. INTRODUCTION

Additive manufacturing (AM) has undergone a major development since its beginning in the 80s. Today, there exist numerous techniques that make it possible to obtain components of different materials with a high degree of complexity and customization without an excessive cost increment. This makes AM of great interest to leading sectors such as aerospace, automotive, medical, etc. Nevertheless, due to the novelty of most of these techniques and the subsequent lack of standardization, quality assurance of the AM parts becomes a key issue today, Tofail et al. (2018). This fact, together with the long manufacturing time required for high value-added parts and as well as the design possibilities provided by this technology, both regarding internal cavities and structures, has led researchers to focus their efforts on the development of different in-situ inspection techniques, which make it possible to analyze each manufactured layer and, therefore, the quality of the parts during the process.

Typically, these in-situ techniques are based on using different types of sensors, Everton et al. (2016), each of which showing different advantages and drawbacks. Charge-Coupled Devices (CCD) are cheap, compact and allow for obtaining high-definition images, but they usually show optical distortions in the captured information due to the type of lenses that they mount, Kannala et al. (2006). Non-contact triangulation laser sensors allow for obtaining high-quality metrological data but are expensive and require more complex digitizing and data-processing procedures, Vasconcelos et al. (2012). Contact Image Sensors (CIS) are compact, cheap and enable fast digitizing of broad surfaces, but problems arise when the contrast of the captured images is below a certain threshold, Blanco et al. (2021). Therefore, exploration of further types of sensors for geometrical errors detection layerwise in AM becomes of great interest nowadays.

A technology that can be applied for this purpose is Conoscopic Holography (CH), a type of incoherent light interferometric technique able to detect the distance between the sensor and the projected laser spot on a surface. For that, CH point-type sensors analyze the light reflected by the surface, which arrives to the sensor's linear CCD via a conoscope, Sirat et al. (2005). This technology can be used on a wide variety of materials, and its high-quality metrological performance was demonstrated, Zapico et al. (2018).

Accordingly, the feasibility of using a CH point-type sensor for AM layer contour error detection is analyzed in this work. For a set of circular geometries obtained by Fused Filament Fabrication (FFF), the performance of the CH sensor is assessed by comparing the measurement results to those obtained with a Coordinate Measuring Machine (CMM) used as ground truth. The CH sensor's performance is also compared with that of a CIS, another digitizing system commonly used by researchers for this error detection purpose.

2. MATERIALS

A point-type CH sensor (ConoPoint-10 by Optimet) equipped with a lens of 50 mm focal length was used in this work. The main specifications of this setup are shown in Table 1. To achieve a relative controlled movement between the sensor and the digitized surface, the CH sensor was integrated into a 3-axis machining center (MC), Zapico et al. (2019).

By using this integrated system, the circular area of the top layers of a set of FFF specimens were digitized. Each specimen consists of an inverted truncated cone standing on a base (Fig. 1). Specimens of three different heights h were used (i.e., 2, 4 and 8 mm).

10.1016/j.ifacol.2022.09.520

Table 1. ConoPoint-10 specifications, Optimet (2017)

Property	50 mm lens
Dimensions (L × W × H) (mm)	167 × 79 × 57
Weight (g)	720
Measurement frequency, F (Hz)	up to 9000
Depth of field, DOF (mm)	8
Stand-off (mm)	44
Repeatability (µm)	0.10
Narrowest spot size (µm)	37

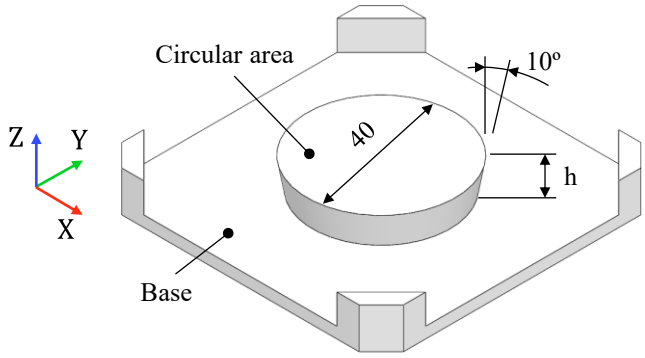

Figure 1. Features of the specimens.

The errors of the circular contour detected with the CH system were compared to those obtained on a DEA Global Image CMM. This machine is equipped with a Renishaw PH10-MQ and a SP25M scanning probe system whose metrological specifications are shown in (1) and (2). In this work, a 2 mm cylindrical shank probe was used to ensure a tangential contact with the specimen's circular area contour.

$$R_{0,MPL} = 2.2\ \mu m \quad (1)$$

$$E_{0,MPE} = 2.2 + 3L \cdot 10^{-3}\ \mu m, \text{being L in mm} \quad (2)$$

The measurement results were also compared to those obtained with a CIS on the same specimens. This sensor is the one of a low-cost flatbed scanner (Perfection V39 by EPSON), with a working area of 216 x 297 mm and different digitizing resolutions up to 4,800 dots-per-inch (dpi). Due to the trademark intellectual property, not much information about internal operation of this sensor is available and only a few setting parameters can be configured.

3. METHODS

3.1 Digitizing

With the aim to perform an effective digitizing task according to the CH sensor characteristics, a radial digitizing routine was developed. The digitizing parameters of the circular contour were the radial digitizing length, L_R, and the angular separation between scanning passes, θ (Fig. 2). In this routine, each radius is centered with the contour thanks to a pre-digitizing alignment procedure. In all the specimens, 4 mm length radii were digitized under two angular separations of 1º and 5º providing two different digitizing densities so-called CH_{HD} and CH_{LD} for CH high density and low density digitizing, respectively.

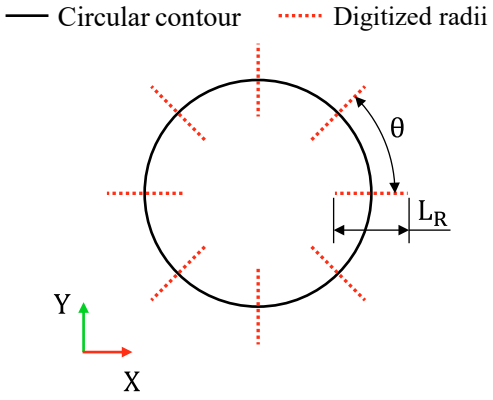

Figure 2. CH digitizing routine of the circular area contour.

For both densities, the CH sensor was configured in a time-trigger mode using ~~a~~ frequency of 6,000 Hz and ~~a~~ power of 22%, ensuring enough quality measurements according to the manufacturer's recommendations, Optimet (2017). The MC feed rate along the radii digitizing was 200 mm/min in order to reduce the system vibrations and, therefore, to obtain more reliable results. A radial digitizing resolution of around 0.6 µm was achieved, which was rounded up to ~~the~~ 1 µm resolution of the MC linear encoders. The digitizing time was about 2 minutes for CH_{LD} and 10 minutes for CH_{HD}.

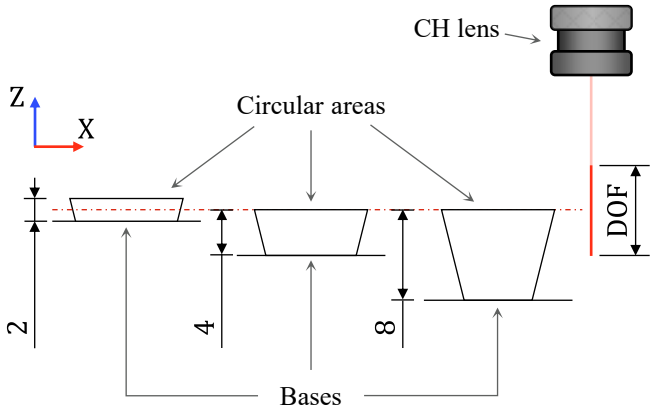

Figure 3. Representation of the relative vertical position between the specimens and the CH sensor during digitizing.

The relative position between the circular area of the specimens and the CH sensor was adjusted so that, in the case of 4 mm and 8 mm height specimens, the circular area matched the middle of the DOF, whereas in the 2 mm specimen the height difference between the circular area and the base was centered in the DOF (Fig. 3). Thus, in the latter specimen the CH sensor was able to provide enough quality digitized points of both the circular area and the base. On the other hand, digitization of the specimens with the CIS was performed using a 2,400 dpi resolution and the default configuration provided by the manufacturer. The digitization took 2 minutes per specimen, similarly to the case of CH_{LD}. In the case of CMM specimens' digitization, 360 points with a homogeneous angular distribution around the circular contour were captured.

3.2 Data processing

Given the point cloud obtained using the CH sensor, several steps must be followed to obtain the contour of the circular area of the specimens. The procedure flowchart is shown in Fig. 4.

First, the point cloud is analyzed to check if more than one surface lies within the DOF and a height clustering procedure is applied in such a case. This procedure involves fitting a *Gaussian Mixture Model* to the distribution of the Z-values of the points. The model will indicate the mean and a dispersion coefficient for each found distribution within the overall data. Once the results are obtained, the surface of interest is extracted.

Then, the extracted point cloud is levelled and shifted to match the XY plane using the *Principal Component Analysis* method. After that, an outlier filter is applied to the data based on the standard deviation on the Z-values distribution.

Finally, the MATLAB® *boundary* detection algorithm is applied to the XY coordinates of the processed point cloud, with a shrinkage factor of 0.25. In this way, the points that lie on the limiting edge of the digitized surface are determined.

Then, a fitting circle was calculated using the contour points and a central point was estimated. Considering this center, points that lie on the contour were obtained at constant angular intervals. The radial position of these points with respect to the nominal contour provide deviations that are later compared to those determined with the CMM.

The processing of the data captured by the CIS was carried out in a previous work by Blanco et al. (2021). The main steps are represented in Fig. 4. Once determined the contour error detected by this sensor, the results were compared to those on the CMM in a similar way than in the CH sensor digitizing cases.

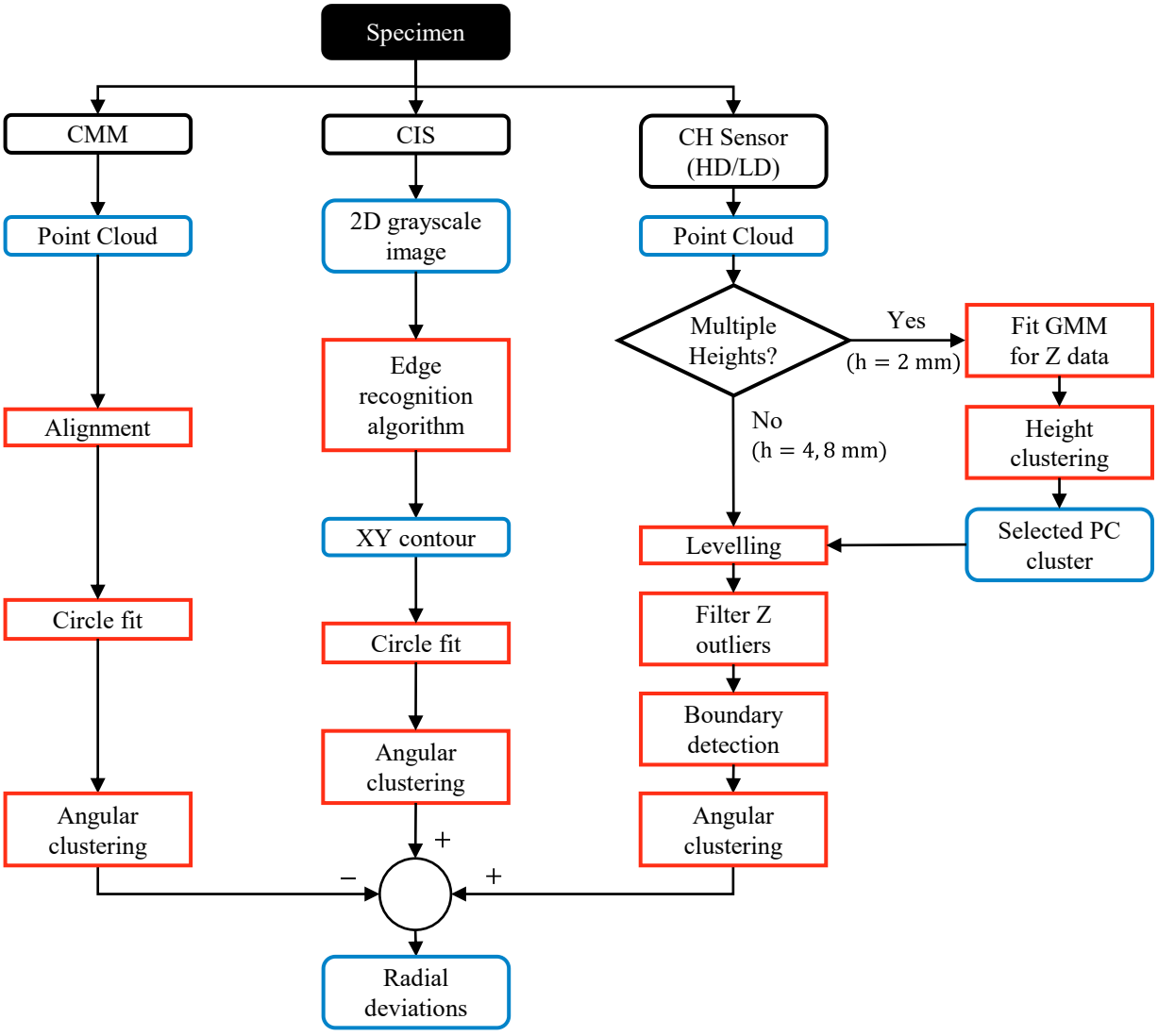

Figure 4. CH point cloud processing flowchart.

4. RESULTS AND DISCUSSION

The form errors detected by the CMM, CIS and CH sensor under both digitizing densities (i.e., CH_{LD} and CH_{HD}), are shown in Fig. 5 (a, c, e) for the specimens of heights 2, 4 and 8 mm, respectively. As it can be noticed observing the CMM results, the circular area contours of the specimens show a general oval-shaped form, probably related to a XY axes squareness defect of the AM machine used. This form has been detected by the two compared sensors (i.e., CH and CIS), but with different performance.

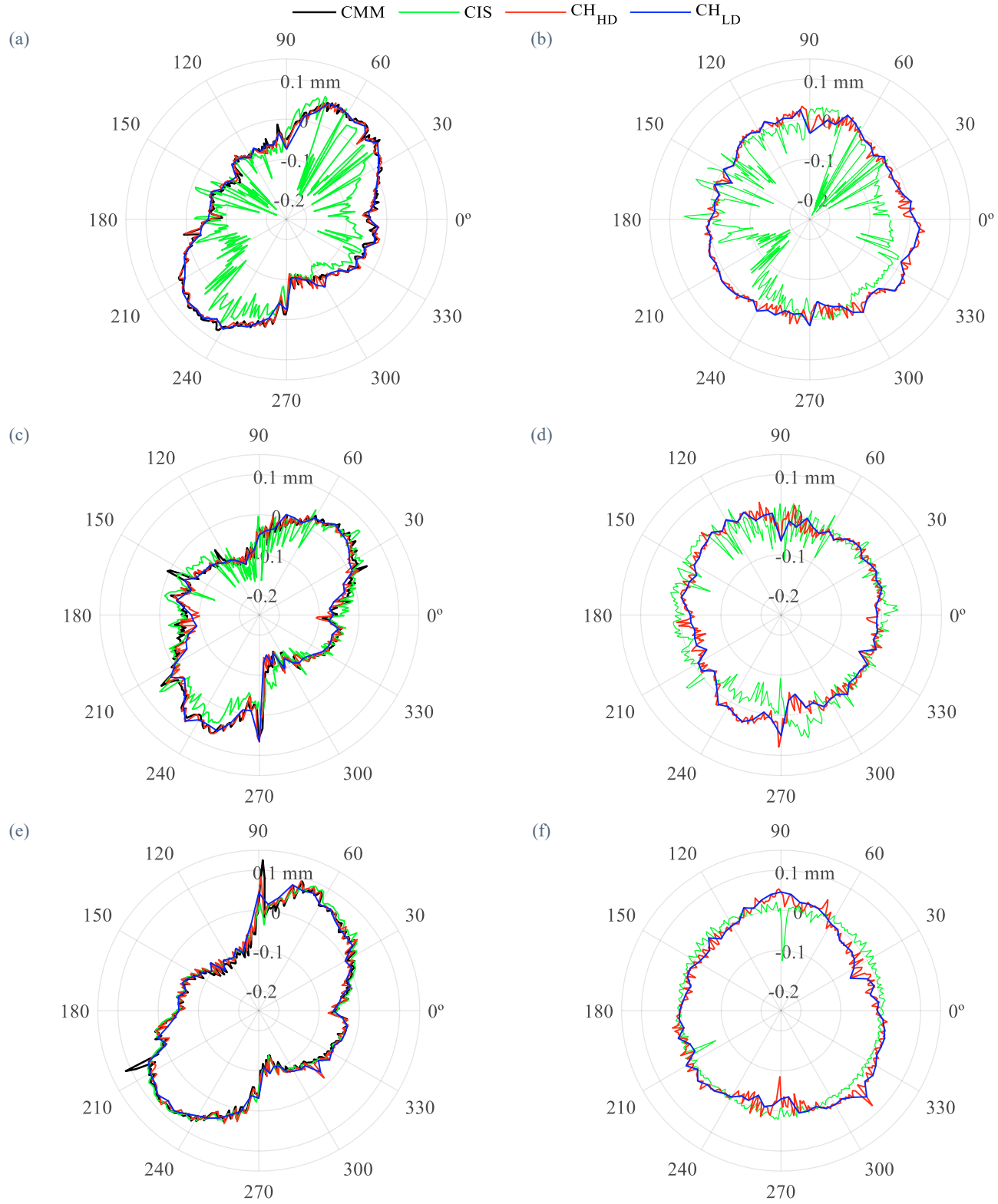

Figure 5. Polar plot of form errors in specimens of heights 2 mm (a), 4 mm (c) and 8 mm (e), and deviations of the data captured with the sensors and different densities with respect to the CMM results – (b), (d), (f) –.

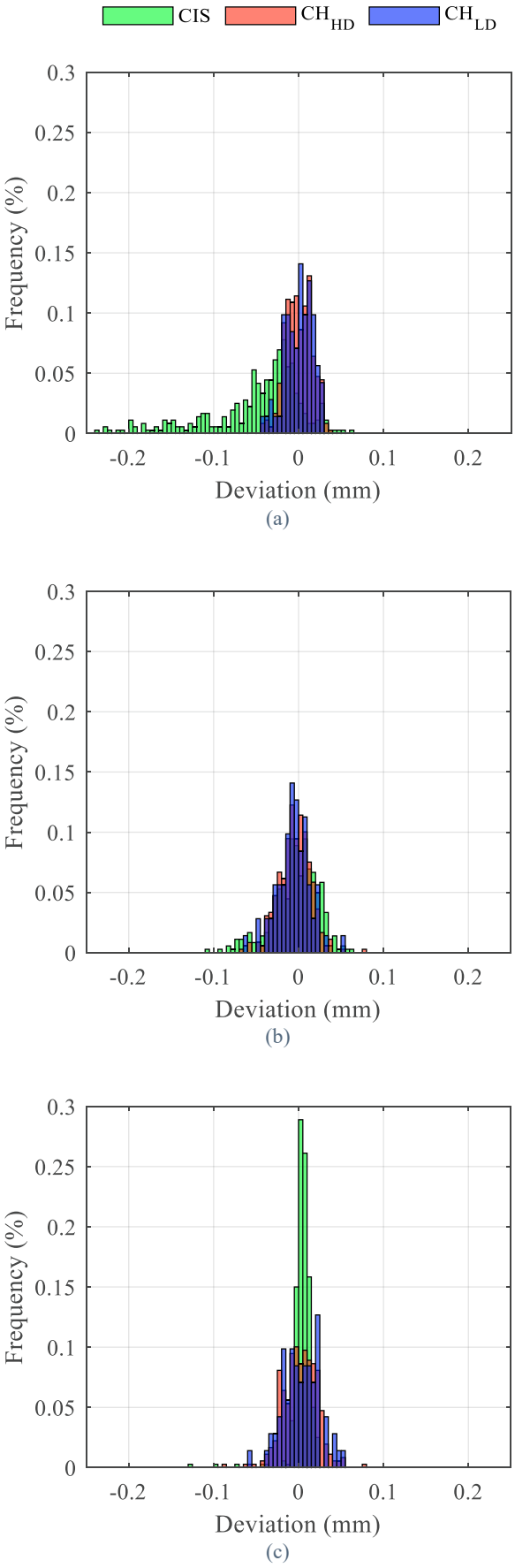

Figure 6. Distribution of form error deviations for specimens of 2 mm (a), 4 mm (b), and 8 mm (c) height.

The different behavior of these sensors with respect to the CMM is shown in Fig. 5 (b, d, f) and Fig. 6 (a, b, c), the latter by means of the error histogram. In the case of the CH sensor, both digitizing densities match deviations detected on the CMM. Despite the low density of the CH_{LD} digitizing, results may be sufficient for a general contour error detection. In the case of the CIS, a strong correlation between the specimen height and the sensor performance can be noticed. The higher the specimen, the better performance of the CIS due to the higher contrast between the circular area and the base that is observed in the images.

Based on the form error deviations observed on the CMM, three quality indicators were calculated: mean deviation, Interquartile Range (IQR), and absolute maximum deviation ($|Dev_{max}|$). The values of these parameters are summarized in Table 2 for both sensors and all specimen heights. In the case of mean deviation, similar results are observed for both sensors and all the specimens, except for the CIS over the 2 mm specimen. Regarding the IQR, while the CH presents a consistent dispersion, the CIS shows an inverse correlation between specimen height and dispersion. On the other hand, the maximum absolute deviations in the case of the CH are systematically lower than in the case of the CIS. Special mention should be made for the value of this indicator corresponding to the 2 mm specimen, which duplicates the values met for the other two specimens with the CIS.

According to this analysis, the CH sensor results are consistent independently of the specimen height and the digitizing strategy developed, although the CIS is more suitable for the 8 mm height.

Table 2. Quality indicators of the measured form error for the different specimens and sensors.

			Mean (µm)	**IQR** (µm)	**$\|Dev_{max}\|$** (µm)
Specimen height	2 mm	CIS	-47.8	53.1	238.2
		CH_{HD}	-0.1	23.4	44.3
		CH_{LD}	0.2	22.4	43.9
	4 mm	CIS	-3.7	33.2	108.3
		CH_{HD}	-4.6	24.3	79.1
		CH_{LD}	-5.6	22.6	64.1
	8 mm	CIS	4.3	8.9	125.4
		CH_{HD}	1.8	27.8	85.5
		CH_{LD}	2.6	30.5	58.5

5. CONCLUSIONS

The feasibility of using a Conoscopic Holography point-type sensor applied to layer contour error detection in Additive Manufacturing processes was analyzed in this work. Two different density digitizing strategies were performed on circular specimens produced by Fused Filament Fabrication. After processing the gathered point clouds, the radial errors between the points on the actual contour and the ones on the nominal circle were calculated. The error results were

compared to those determined by measuring the same specimens on a CMM (considered as ground truth) and also by means of a low-cost Contact Image Sensor (commonly used for in-situ monitoring tasks). Three quantitative quality indicators were analyzed: one for the mean deviation, another for deviation dispersion (interquartile range − IQR) and the last one for the absolute maximum deviation.

A fine coincidence was found between the three measurement technologies regarding the general form deviations (e.g, ovality in this case) but, regarding the contour radial deviations, a finer similarity was found between the CH sensor and the CMM. Moreover, both digitizing densities showed similar indicator values for the specimen of the three heights considered. In the case of the CIS, deviations with respect to the CMM increased as the height parameter decreased due to the lower contrast found between the image areas corresponding to the top and the bottom specimen surfaces. This was stated according to the inverse correlation between the quality indicators values and the height of the specimen.

In conclusion, it can be stated that the CH sensor provides reliable results in assessing the form deviations layerwise in AM parts. Although the point-type sensor used in this work would require an optimization of both density and scanning strategy to minimize the digitizing time, this drawback could be avoided by using a line-type CH sensor instead. Further investigations regarding to the efficiency-cost relationship would be necessary to take a decision in this way.

ACKNOWLEDGEMENTS

This work is supported by the Spanish Ministry of Economy, Industry and Competitiveness and FEDER (DPI2017-83068-P).

REFERENCES

Blanco, D., Fernández, P., Fernández, A., Alvarez, B.J. and Rico, J.C. (2021). The Influence of Image Processing and Layer-to-Background Contrast on the Reliability of Flatbed Scanner-Based Characterisation of Additively Manufactured Layer Contours. *Applied Sciences*, 11(1), 178.

Everton, S.K., Hirsch, M., Stravroulakis, P., Leach, R.K. and Clare, A.T. (2016). Review of in-situ process monitoring and in-situ metrology for metal additive manufacturing. *Materials & Design*, 95, 431-445.

Kannala, J. and Brandt, S.S. (2006). A generic camera model and calibration method for conventional, wide-angle, and fish-eye lenses. *IEEE transactions on pattern analysis and machine intelligence*, 28(8), 1335-1340.

Optimet (2017), ConoPoint Series User Manual (P/N 3J06009). Optimet OPHIR Photonics, Israel.

Sirat, G.Y., Paz, F., Agronik, G. and Wilner, K. (2005). Conoscopic systems and conoscopic holography. Optimet, Israel.

Tofail, S.A., Koumoulos, E.P., Bandyopadhyay, A., Bose, S., O'Donoghue, L. and Charitidis, C. (2018). Additive manufacturing: scientific and technological challenges, market uptake and opportunities. *Materials today*, 21(1), 22-37.

Vasconcelos, F., Barreto, J.P. and Nunes, U. (2012). A minimal solution for the extrinsic calibration of a camera and a laser-rangefinder. *IEEE transactions on pattern analysis and machine intelligence*, 34(11), 2097-2107.

Zapico, P., Fernández, P., Rico, J.C., Valiño, G. and Patiño, H. (2018). Extrinsic calibration of a conoscopic holography system integrated in a CMM. *Precision Engineering*, 52, 484-493.

Zapico, P., Patiño, H., Valiño, G., Fernández, P. and Rico, J.C. (2019). CNC centralized control for digitizing freeform surfaces by means of a conoscopic holography sensor integrated in a machining centre. *Precision Engineering*, 55, 474-483.